Biomedical Informatics Insights

ORIGINAL RESEARCH

Differential Transcriptional Changes in Mice Exposed to Chemically Distinct Diesel Samples

Tina Stevens[1], Susan Hester[2] and M. Ian Gilmour[1]

[1]Environmental Public Health Division and [2]Integrated Systems Toxicology Division, National Health and Environmental Effects Research Laboratory, U.S. Environmental Protection Agency, Research Triangle Park, North Carolina, 27711, USA. Corresponding author email: gilmour.ian@epa.gov

Abstract: Epidemiological studies have linked exposure to ambient particulate matter (PM) with increased asthmatic symptoms. Diesel exhaust particles (DEP) are a predominant source of vehicle derived ambient PM, and experimental studies have demonstrated that they may have adjuvant potential when given with an antigen. We previously compared 3 DEP samples: N-DEP, A-DEP, and C-DEP in a murine ovalbumin (OVA) mucosal sensitization model and reported the adjuvant activity to be: C-DEP ≈ A-DEP > N-DEP. The present study analyzed gene expression changes from the lungs of these mice. Transcription profiling demonstrated that all the DEP samples altered cytokine and toll-like receptor pathways regardless of type, with or without antigen sensitization. Further analysis of DEP exposure with OVA showed that all DEP treatments altered networks involved in immune and inflammatory responses. The A- and C-DEP/OVA treatments induced differential expression of apoptosis pathways in association with stronger adjuvant responses, while expression of cell cycle control and DNA damage pathways were also altered in the C-DEP/OVA treatment. This comprehensive approach using gene expression analysis to examine changes at a pathway level provides detailed information on events occurring in the lung after DEP exposure, and confirms that the most bioactive sample induced many more individual genes and changes in immuno-regulatory and homeostatic pathways.

Keywords: diesel exhaust particles, allergy, inflammation, lung, genomics, mouse model

Biomedical Informatics Insights 2010:3 29–52

This article is available from http://www.la-press.com.

Introduction

Epidemiology studies have reported an association between increased ambient particle matter (PM) levels and hospital admission rates due to respiratory illnesses including asthma.[1] Diesel exhaust particles (DEP) are an important contributor to ambient PM and many studies have focused on DEP as a model anthropogenic pollutant. DEP consist of a carbon core surrounded by various amounts of adsorbed organic compounds, including polycyclic aromatic hydrocarbons (PAHs), quinones, and nitro-PAHs.[2] Human and rodent studies have shown that DEP augments the induction of allergic lung disease when given with an antigen.[3–6] Although the chemical composition and biologic mechanisms associated with the adjuvant effects of DEP are not well understood, the organic components of DEP and resulting oxidative stress responses are thought to skew the immune system towards a T-helper 2 (T_H2) response.[7–10]

The composition of DEP varies greatly depending on the type of engine, load, and method of collection, which in turn can alter its biological function. Singh et al[8] investigated the chemical characteristics and pulmonary toxicity of two different particles, an automobile derived DEP (A-DEP) and National Institute of Standard Technology standard reference material 2975 (N-DEP) generated from a heavy forklift. The two particle samples exhibited disparate pulmonary toxicity and mutagenic activity, which reflected their dissimilar chemical composition. Recently, we assessed the effects of N-DEP, A-DEP, and a newer particle termed C-DEP (generated from a diesel engine used to power a compressor) in a murine ovalbumin (OVA) mucosal sensitization model.[11] These samples differed in their percentage of dichloromethane (DCM) extractable organic material (EOM) and PAHs with N-DEP, C-DEP, and A-DEP containing 1.5%, 18.9%, and 67% EOM, and 47, 431, and 522 μg of PAHs per gram of DEP, respectively. Immune and inflammatory endpoints demonstrated the degree of allergic adjuvancy as follows: C-DEP/OVA ≈ A-DEP/OVA >> N-DEP/OVA suggesting that the amount of PAHs rather than the total organic content tracked with adjuvant activity. Consistent with this strong degree of adjuvancy post-challenge, the C-DEP exposure at sensitization increased the influx of eosinophils, neutrophils, and lymphocytes, and the production of T_H2 cytokines, while reducing levels of the T_H1 cytokine IL-12 in the BALF.[11] In contrast, the elemental carbon rich N-DEP/OVA induced a milder T_H2 phenotype post-sensitization while the A-DEP did not alter measured post-sensitization values, but displayed strong adjuvant activities post-challenge.[11]

We have previously demonstrated that inhalation exposure to fresh diesel exhaust (DE) from the same engine that produced the C-DEP sample at an occupationally relevant dose, caused mild adjuvant effects compared to air controls.[12] Global gene expression analysis showed that the DE in combination with OVA sensitization altered oxidative stress and metabolism pathways, whereas DE in the absence of immunization modulated cell cycle control, growth and differentiation, G-proteins, and cell adhesion pathways. To understand more precisely which pathways and cellular signaling events were amplified by the three chemically distinct DEP samples during sensitization, we initiated a similar global genomic approach. Microarray analysis of whole-lung RNA was used to elucidate the pathways and networks involved in the effects of N-DEP, A-DEP, and C-DEP with or without allergen sensitization in BALB/C mice. The design of the study permitted direct comparison of early global gene expression changes with the previously reported pulmonary immune and inflammatory effects of DEP alone and in combination with OVA.

Materials and Methods

Animals

Female BALB/C mice (8–10 weeks old) were obtained from Charles River Laboratories (Raleigh, NC) and allowed to acclimate for a minimum of one week prior to dosing. Mice were randomly assigned to treatment groups and housed in an AAALAC-approved animal facility at the US-EPA. All animal procedures were reviewed and approved by the US-EPA's Institutional Animal Care and Use Committee. Housing environment conditions include a 12-h light/dark cycle at an ambient temperature of 22 ± 1 °C and relative humidity of 55 ± 5 °C. Mice were provided water and mouse chow *ad libitum*. Additional mice from each facility were routinely monitored serologically for Sendai, mouse pneumonia, mouse hepatitis, and other murine viruses, as well as mycoplasma.

Particle samples

Standard Reference Material (SRM) 2975 diesel exhaust particle sample (N-DEP) was purchased from National Institute of Standard Technology (NIST) (Gaithersburg, MD). The reported mean diameter of these particles was 11.2 ± 0.1 μm by area distribution, and the surface area, as determined by nitrogen adsorption, was 91 $\mu m^2/g$. The certified analysis contains 11 certified concentrations and 28 reference concentrations for selected PAHs found in the DEPs. The DEP was generated by a heavy-duty forklift diesel engine and collected under "hot" conditions without a dilution tunnel.

Automobile DEP (A-DEP; courtesy of T. Kobayashi, NIES, Japan) was generated and collected under conditions previously described.[13,14] Briefly, the sample was generated by a light-duty (2740 cc), 4-cylinder Isuzu diesel engine. DEP was collected under "cold" (50 °C) conditions onto glass-fiber filters and on steel duct walls in a constant-volume sampling system fitted at the end of a dilution tunnel.

Compressor DEP (C-DEP) was generated in-house as described by Cao et al[15] at the EPA using a 30 kW (40 hp) 4-cylinder Deutz BF4M1008 diesel engine connected to a 22.3 kW Saylor Bell air compressor to provide 20% load. The generated particles were collected under "hot" conditions in a baghouse.

Experimental design

DEP samples (N-, C-, A-DEP) were suspended at a concentration of 3 mg/ml in saline alone or with 0.4 mg/ml of OVA. Particles were sonicated using a Microson Ultrasonic Cell Disruptor (Micromix) for 10 min. Mice were randomly divided into 8 treatment groups containing 5 mice each, anesthetized with isofluorane, and exposed to saline, 20 μg OVA, 150 μg DEP, or DEP + OVA by intranasal instillation on Days 0 and 13 and necropsied 18 hrs later. Additional groups of animals were held for subsequent phenotypic analysis post-challenge.

Necropsy and RNA isolation

Mice were euthanized with sodium pentobarbital and bled by cardiac puncture. The chest wall was opened and the left lung lobe was removed, quick frozen in liquid nitrogen, and stored at −80 °C. RNA from frozen lung tissue was isolated using RNeasy (Qiagen, Valencia, CA) following manufacturer's protocol. Quantity and quality of the RNA was measured using a Nanospot and Agilent Bioanalyzer (Agilent Technologies, Palo Alto, CA), respectively. Three mice were randomly selected from each group of five animals for microarray analysis.

Microarray

RNA samples were selected prepared, processed, and hybridized to the Affymetrix Mouse 430 A gene chip at Expression Analysis (Durham, NC), as described in the GeneChip Expression Analysis Manual (Affymetrix; Santa Clara, CA). The hybridized probe array was stained with streptavidin phycoerythrin conjugate and scanned by the GeneChip® Scanner 3000 (Affymetrix; Santa Clara, CA). The amount of light emitted at 570 nm is proportional to the bound target at each location on the probe array.

The Mouse 430 A Genome chip contains over 22,000 probe sets representing over 14,000 well-characterized mouse genes. A detailed description can be found at http://www.affymetrix.com/products/arrays/specific/mouse430.affx. A total of 24 gene chips representing lung samples from 24 individual mice (8 treatments, N = 3) were used in this study. The microarray data have been deposited at Genome Expression Omnibus database (http://www.ncbi.nlm.nih.gov/geo/) and are accessible through GEO series accession number GSE22357.

Overall data analysis strategy

The analysis approach of this data set, consisting of 2 controls and 6 treatment groups, was to use a binary comparison approach of each treatment group compared to its respective control: N-DEP and saline, A-DEP and saline, C-DEP and saline, N-DEP/OVA and OVA, A-DEP/OVA and OVA, and C-DEP/OVA and OVA. The analysis of these data sets consisted of: 1) evaluating the data quality; 2) performing principal components analysis (PCA) for a global inspection of within group sample correspondence and to examine model and dose effects; 3) performing Gene Set Enrichment Analysis (GSEA) to determine differentially expressed gene sets between a treatment group and its control; 4) extracting core genes responsible for a particular gene set identified as significant from the

GSEA analysis; 5) determining common differentially expressed genes across treatment groups; 6) mapping core genes to functional pathways using KEGG pathways and MetaCore GENEGO® to identify altered pathways and networks unique or in common among the treatments.

Principal component analysis (PCA)

PCA transforms microarray data from all gene chips to a new coordinate system using an orthogonal linear transformation, which identifies a lower dimensional coordinate system that accounts for most of the variance in the data set. This analysis was employed to survey the data for within-group outliers and model and dose effects using Rosetta Resolver (Rosetta Inpharmatics, Agilent Technologies, Palo Alto, CA) following linear weighting normalization ($P < 0.001$). Each individual gene chip or gene expression profile was represented by a single data point and the variance between a pair of gene chips was comparable to the distance between the data points. The closer the data points the greater the similarity of their gene expression profiles. This analysis was employed as a visual tool to initially inspect the data for within group and across group similarities and dissimilarities.

Gene set enrichment analysis (GSEA)

GSEA is a powerful computational method that utilizes an *a priori* defined set of genes to determine statistically significant, concordant differences between two phenotypes. For this analysis, probe-level data from 24 gene chips were imported into Gene Pattern (www.genepattern.org) and preprocessed using the Robust Multichip Average (RMA) method, which uses background correction, quantile normalization, and median scaling to generate estimated expression summaries.[16] The RMA generated values were imported into GSEA to determine gene sets associated with each diesel treatment group compared to its respective control. The molecular signature database (MSigDB) C2 provided on the website http://www.broad.mit.edu/gsea/msigdb/msigdbindex.html, which contains 1687 gene sets, was queried for association with a particular treatment in each pairwise comparison (N-DEP/OVA and OVA, A-DEP/OVA and OVA, C-DEP/OVA and OVA, N-DEP and saline, A-DEP and saline, and C-DEP and saline). Only gene sets with a minimal gene set size of 15 genes per pathway and a maximum of 90 were queried. We acknowledge our use of GSEA software and MSigDB (http://www.broad.mit.edu/gsea/).[17]

Pathway level analysis

The gene sets with a false discovery rate (FDR) q-value of <0.01 were used to create a core gene list. The core gene list is comprised of genes responsible for a gene set being considered significant. These genes were exported and then applied to two pathway analysis programs, KEGG Pathway Analysis (http://gather.genome.duke.edu/) and MetaCore GENEGO® (http://www.genego.com/metacore), which maps genes to pathways and determines pathway significance. All pathways with a *P*-value of <0.001 and at least 5 or more differentially expressed genes were reported.

Results

Principal component analysis (PCA)

PCA was applied to provide a multidimensional gene expression profile of each gene chip in a 3 dimensional space to reveal clusters in the experimental data. All data from the 24 gene chips were analyzed with each dot representing a gene chip (Fig. 1a). After analysis the gene chips were then highlighted in either blue (OVA treatment) or red (saline control). Good separation of the two groups was observed, illustrating a model effect between antigen and saline. The saline group appeared to be more tightly clustered than OVA indicating lower within group variability. To determine if exposure to chemically different DEP samples induces diverse genetic profiles, the gene chips were highlighted according to diesel sample (purple- A-DEP and A-DEP/OVA, blue- C-DEP and C-DEP/OVA, green- N-DEP and N-DEP/OVA, and yellow- saline and OVA) (Fig. 1b). The plot revealed separation of the saline and OVA treated C-DEP and N-DEP groups, while the saline and OVA A-DEP exposed mice clustered together.

Gene set enrichment analysis (GSEA)

GSEA was developed to overcome the limitations of relatively small individual differential gene expression changes among biologically related genes and small sample size. In contrast to conventional microarray analysis programs, the algorithm employed by GSEA derives its power by focusing on gene sets with biological relevance rather than individual genes.[17,18]

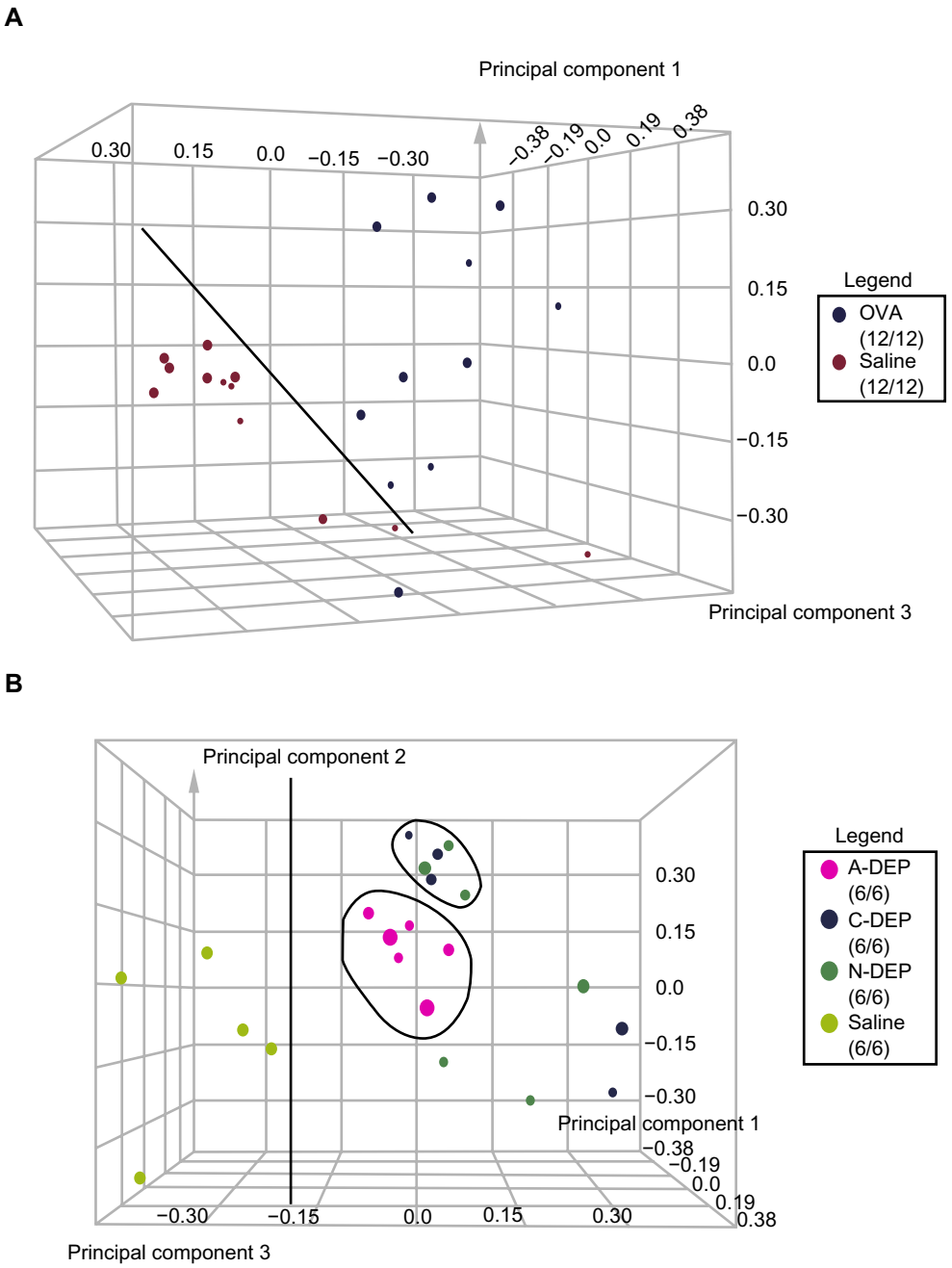

Figure 1. Principle component analysis (PCA) plot from microarray data. PCA plots were created in Rosetta Resolver. Each plot is a representation of all gene chip samples (8 treatments, n = 3) and each dot represents all the genes from one gene chip. Gene chips were highlighted according to the immunization protocol (**A**) (blue-OVA treatment or red-saline treatment) or the diesel exposure (**B**) (yellow- saline and saline/OVA, pink- A-DEP and A-DEP/OVA, blue- C-DEP/saline and C-DEP/OVA, and green- N-DEP/saline and N-DEP/OVA).

To test for sets of related genes that were altered in the lungs of mice exposed to the various treatments, we employed GSEA. The arrays were separated into 6 binary groups; N-DEP/saline and saline, A-DEP/saline and saline, C-DEP/saline and saline, N-DEP/OVA and OVA, A-DEP/OVA and OVA, and C-DEP/OVA and OVA. The C2 collection of curated gene sets from the MSigDB were queried and a detailed description of each gene set can be found on the website http://www.broad.mit.edu/gsea/msigdb/msigdb_zindex.html. Gene sets with an FDR q-value of <0.01 were considered significant. The number of significant gene sets associated with N-DEP, A-DEP, and C-DEP, as determined by the pairwise comparisons (DEP exposure and saline control), was 101, 90, and 98, respectively. In the context of antigen,

60, 68, and 113 gene sets were associated with N-, A-, and C-DEP/OVA, respectively. The complete list of the significant gene sets is found in Appendices 1–6.

Venn analyses

Venn analyses were performed to identify the common genes to all DEP exposures. The core genes (those genes responsible for a gene set being considered significant with an FDR q-values of <0.01) were extracted from the significant gene sets associated with each diesel exposure identified by GSEA. A Venn diagram was constructed to identify genes common among the 3 DEP/saline exposure pairwise comparisons (Fig. 2a). A-DEP/saline exposure resulted in the greatest number of differentially expressed genes (545). 200 genes were common among all 3 DEP treatments. Similarly a Venn diagram was constructed for the genes associated with each DEP/OVA exposure (Fig. 2b). C-DEP/OVA exposure resulted in greatest number of differentially expressed genes (800). 236 genes were found common to all DEP/OVA exposures. The two sets of common genes were applied to another Venn diagram to identify the 117 common genes among all DEP exposures (Fig. 2c).

KEGG pathway analyses

To understand the biological significance of the common genes associated with the 3 DEP/saline exposures, the 200 genes were imported into the gene annotation tool, Gather (http://gather.genome.duke.edu/), and the genes were mapped to KEGG pathways, using the criteria that pathways must have 5 or more differentially expressed genes and be over-represented based on a hypergeometric test with a *P*-value <0.001. Cytokine-cytokine receptor interaction and toll-like receptor signaling pathways were common to all DEP/saline exposures (Table 1) with the majority of the genes being associated with neutrophil signaling. The 236 genes common among the 3 DEP/OVA exposures also significantly populated the cytokine-cytokine receptor interaction and toll-like receptor (TLR) signaling pathway (Table 2), but with better coverage of these pathways (40 and 17 genes for DEP/OVA versus 28 and 11 genes for DEP/saline, respectively). In addition the DEP/OVA treatments also significantly altered 11 genes associated with apoptosis pathways (Table 2).

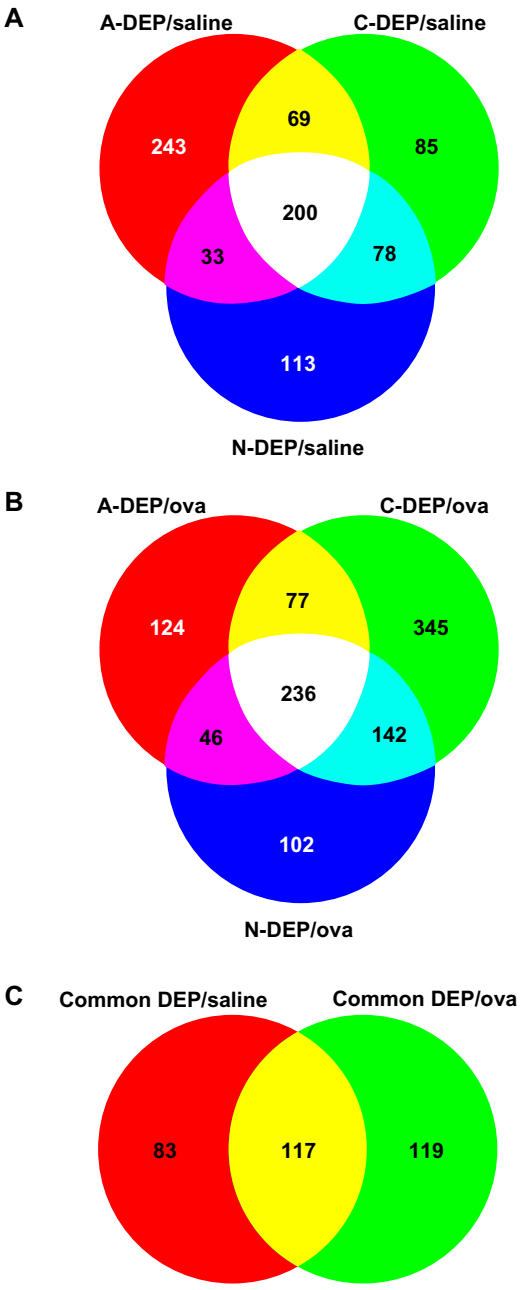

Figure 2. Venn analyses. Venn analyses of the core genes extracted from significantly altered gene sets in GSEA associated with A-, C-, and N-DEP/saline exposures (**A**) and A-, C-, N-DEP/OVA exposurse (**B**). Venn analysis of the common genes associated with all DEP/saline and DEP/OVA exposures (**C**).

To understand the effects of the individual DEP/OVA exposures, the extracted core genes were mapped to KEGG pathways and the results represented in Tables 4–6. All 3 exposures populated the cytokine-cytokine receptor pathway similarly with 56, 56, and 51 genes for N-DEP/OVA, A-DEP/OVA, and C-DEP/OVA, respectively. Additionally, the TLR pathway

Table 1. KEGG pathways mapped from the 200 common genes associated with DEP/saline exposure.

KEGG pathway	# Genes	*P* value
Cytokine-cytokine receptor interaction Ccl17 Ccl2 Ccl22 Ccl3 Ccl4 Ccl6 Ccl7 Ccl8 Ccl9 Ccr1 Ccr2 Csf2 Csf2rb1 Cxcl1 Cxcl10 Cxcl13 Cxcl2 Cxcl5 Ifngr2 Il1b Il1r2 Il8rb Inhba Ltb Osmr Tnf Tnfrsf1b Tnfrsf9	28	<0.0001
Toll-like receptor signaling pathway Ccl3 Ccl4 Cd14 Cxcl10 Il1b Nfkb2 Nfkbia Pik3cd Rac2 Tlr2 Tnf	11	<0.0001

Table 2. KEGG pathways mapped from the 236 genes common to all DEP/OVA exposure.

KEGG pathway	# Genes	*P* value
Cytokine-cytokine receptor interaction Ccl11 Ccl17 Ccl2 Ccl22 Ccl3 Ccl4 Ccl6 Ccl7 Ccl8 Ccl9 Ccr1 Ccr2 Ccr5 Csf1 Csf2 Csf2ra Csf2rb1 Csf2rb2 Csf3r Cxcl1 Cxcl10 Cxcl11 Cxcl13 Cxcl2 Cxcl5 Cxcl9 Ifngr2 Il1a Il1b Il1r1 Il1r2 Il2rg Il6 Il8rb Osmr Tgfb1 Tnf Tnfrsf1b Tnfrsf5 Tnfrsf9	40	<0.0001
Toll-like receptor signaling pathway Ccl3 Ccl4 Cd14 Cxcl10 Cxcl11 Cxcl9 Ikbke Il1b Il6 Lbp Nfkb1 Nfkb2 Pik3cd Rac2 Stat1 Tlr2 Tnf	17	<0.0001
Apoptosis Birc3 Cflar Csf2rb1 Csf2rb2 Il1a Il1b Il1r1 Nfkb1 Nfkb2 Pik3cd Tnf	11	0.0002

Table 3. KEGG pathways mapped from the 117 genes common to both DEP/OVA and DEP/saline exposure.

KEGG pathway	# Genes	*P* value
Cytokine-cytokine receptor interaction Ccl17 Ccl2 Ccl22 Ccl3 Ccl4 Ccl6 Ccl7 Ccl8 Ccl9 Ccr1 Ccr2 Csf2 Csf2rb1 Cxcl1 Cxcl10 Cxcl13 Cxcl2 Cxcl5 Ifngr2 Il1b Il1r2 Il8rb Osmr Tnf Tnfrsf1b Tnfrsf9	26	<0.0001
Toll-like receptor signaling pathway Ccl3 Ccl4 Cd14 Cxcl10 Il1b Nfkb2 Pik3cd Rac2 Tlr2 Tnf	10	<0.0001

Table 4. KEGG pathway mapped from the 526 genes associated with N-DEP/OVA exposure.

KEGG pathway	# Genes	*P* value
Cytokine-cytokine receptor interaction Ccl11 Ccl17 Ccl2 Ccl22 Ccl3 Ccl4 Ccl6 Ccl7 Ccl8 Ccl9 Ccr1 Ccr2 Ccr5 Ccr6 Ccr7 Csf1 Csf1r Csf2 Csf2ra Csf2rb1 Csf2rb2 Csf3r Cxcl1 Cxcl10 Cxcl11 Cxcl13 Cxcl2 Cxcl5 Cxcl9 Ifnar1 Ifnar2 Ifngr2 Il10ra Il15 Il18rap Il1a Il1b Il1r1 Il1r2 Il2 Il2ra Il2rg Il3ra Il6 Il7r Il8rb Ltb Osmr Tgfb1 Tnf Tnfrsf10b Tnfrsf13c Tnfrsf1b Tnfrsf5 Tnfrsf9 Tnfsf9	56	<0.0001
Toll-like receptor signaling pathway Ccl3 Ccl4 Cd14 Cd86 Cxcl10 Cxcl11 Cxcl9 Fos Ifnar1 Ifnar2 Ikbke Il1b Il6 Lbp Nfkb1 Nfkb2 Nfkbia Pik3cd Rac2 Stat1 Tlr2 Tlr7 Tnf	23	<0.0001
Neuroactive ligand-receptor interaction Adora2b C3ar1 Ctsg Fpr1 P2ry6 Ptger4	6	0.0002

Table 5. KEGG pathways mapped from the 483 genes associated with A-DEP/OVA exposure.

KEGG pathway	# Genes	*P* value
Cytokine-cytokine receptor interaction Ccl11 Ccl17 Ccl2 Ccl22 Ccl3 Ccl4 Ccl6 Ccl7 Ccl8 Ccl9 Ccr1 Ccr2 Ccr4 Ccr5 Csf1 Csf2 Csf2ra Csf2rb1 Csf2rb2 Csf3r Cxcl1 Cxcl10 Cxcl11 Cxcl13 Cxcl2 Cxcl5 Cxcl9 Ifnar2 Ifnb1 Ifng Ifngr2 Il12a Il12b Il12rb1 Il1a Il1b Il1r1 Il1r2 Il2 Il2rg Il4 Il5 Il6 Il8rb Inhba Osmr Tgfb1 Tgfbr1 Tnf Tnfrsf1a Tnfrsf1b Tnfrsf5 Tnfrsf9 Tnfsf10 Tnfsf13 Tnfsf13b	56	<0.0001
Toll-like receptor signaling pathway Ccl3 Ccl4 Cd14 Cxcl10 Cxcl11 Cxcl9 Ifnar2 Ifnb1 Ikbke Il12a Il12b Il1b Il6 Lbp Map3k7ip1 Mapk13 Myd88 Nfkb1 Nfkb2 Nfkbia Pik3cd Rac2 Stat1 Tlr1 Tlr2 Tnf	26	<0.0001
Apoptosis Bax Birc3 Capn1 Casp3 Cflar Csf2rb1 Csf2rb2 Il1a Il1b Il1r1 Myd88 Nfkb1 Nfkb2 Nfkbia Pik3cd Ripk1 Tnf Tnfrsf1a Tnfsf10	19	<0.0001

contained similar amounts of genes with 23, 26, and 28 genes for N-DEP/OVA, A-DEP/OVA, and C-DEP/OVA, respectively. This pathway contained TLRs as well as many pro-inflammatory cytokines and transcription factors. N-DEP/OVA and C-DEP/OVA altered the expression of genes in the neuroactive ligand-receptor interaction pathway. A-DEP/OVA and C-DEP/OVA also altered the apoptosis pathway, while additional pathways for pyrimidine metabolism and aminoacyl-tRNA biosynthesis were unique to the C-DEP/OVA exposures.

GeneGo analysis

The C-DEP/OVA exposure gave the highest transcriptional changes based on the numbers of significant gene sets, extracted core genes, and the KEGG

Table 6. KEGG pathways mapped from the 800 genes associated with C-DEP/OVA exposure.

KEGG pathway	# Genes	*P* value
Apoptosis Apaf1 Bax Bid Birc2 Birc3 Casp3 Casp7 Casp8 Cflar Chuk Csf2rb1 Csf2rb2 Dffa Ikbkb Il1a Il1b Il1r1 Il3ra Irak1 Myd88 Nfkb1 Nfkb2 Pik3cd Ripk1 Tnf Tnfrsf1a Tradd Traf2	28	<0.0001
Cytokine-cytokine receptor interaction Ccl11 Ccl17 Ccl2 Ccl22 Ccl3 Ccl4 Ccl6 Ccl7 Ccl8 Ccl9 Ccr1 Ccr2 Ccr5 Csf1 Csf2 Csf2ra Csf2rb1 Csf2rb2 Csf3r Cxcl1 Cxcl10 Cxcl11 Cxcl13 Cxcl2 Cxcl5 Cxcl9 Ifngr2 Il10ra Il1a Il1b Il1r1 Il1r2 Il2rb Il2rg Il3ra Il6 Il7r Il8rb Inhba Ltb Osmr Tgfb1 Tgfbr1 Tnf Tnfrsf1a Tnfrsf1b Tnfrsf25 Tnfrsf5 Tnfrsf9 Tnfsf13b Tnfsf9	51	<0.0001
Aminoacyl-tRNA biosynthesis Aars Cars Fars1 Farslb Gars Iars Kars Nars Rars Tars Vars2 Wars Yars	13	<0.0001
Toll-like receptor signaling pathway Casp8 Ccl3 Ccl4 Cd14 Chuk Cxcl10 Cxcl11 Cxcl9 Ikbkb Ikbke Il1b Il6 Irak1 Lbp Ly96 Map2k4 Map3k7 Mapk13 Myd88 Nfkb1 Nfkb2 Pik3cd Rac2 Stat1 Tlr2 Tlr4 Tlr7 Tnf	28	<0.0001
Pyrimidine metabolism Ctps Dck Dtymk Dut Ecgf1 Nme1 Nme2 Pola2 Pold1 Pold2 Pole2 Polr2 g Polr2h Polr3k Prim1 Rrm2 Txnrd1 Umpk Umps Upp1	21	<0.0001
Neuroactive ligand-receptor interaction Adora2b Bzrp C3ar1 Grik5 Gzma P2ry6 Ptger4	7	<0.0001

pathways, however, these analyses were not specific enough to allow an inference as to why or how C-DEP was able to elicit a stronger T_H2 response post-sensitization. We therefore mapped the 3 sets of genes to GeneGo curated databases and presented the results as networks and pathways. Figure 3 depicts the significance (-log(p)values) of the top 20 differentially affected GeneGo process networks for all 3 DEP/OVA exposures (N-DEP/OVA-blue; A-DEP/OVA-red; C-DEP/OVA-orange). Using this approach the similarities and differences of the groups can be clearly discerned. All groups significantly altered networks related to antigen presentation, inflammation, and cell adhesion. In addition the C-DEP/OVA exposure also altered networks related to cell cycle control, DNA damage, and protein degradation.

GeneGo pathway analysis revealed that the pathways common to all treatments were associated with MHC class I antigen presentation, inflammation, and other pathways related to the innate immune response. The A-DEP/OVA and C-DEP/OVA common pathways were involved with TNF-α mediated apoptosis pathways whereas C-DEP/OVA alone also induced altered expression of Fas, inhibitor of apoptosis (IAP), and mitochondrial mediated apoptosis and cell cycle regulation pathways (Fig. 4).

Discussion

DEP have been reported to act as adjuvants to upregulate immune responses resulting in increased allergic lung disease; however, there is still a lack of understanding as to what DEP component or components are responsible for these effects, and the underlying mechanisms through which they act. The present study examined global transcriptional changes in the lungs of mice after exposure to three chemically distinct DEP samples (N-, A- and C-DEP) with or without antigen sensitization. Overall, all the DEP and DEP/OVA samples significantly altered cytokine and TLR pathways compared to their respective controls, however, the DEP/OVA samples induced a greater number of genes in these pathways. In addition,

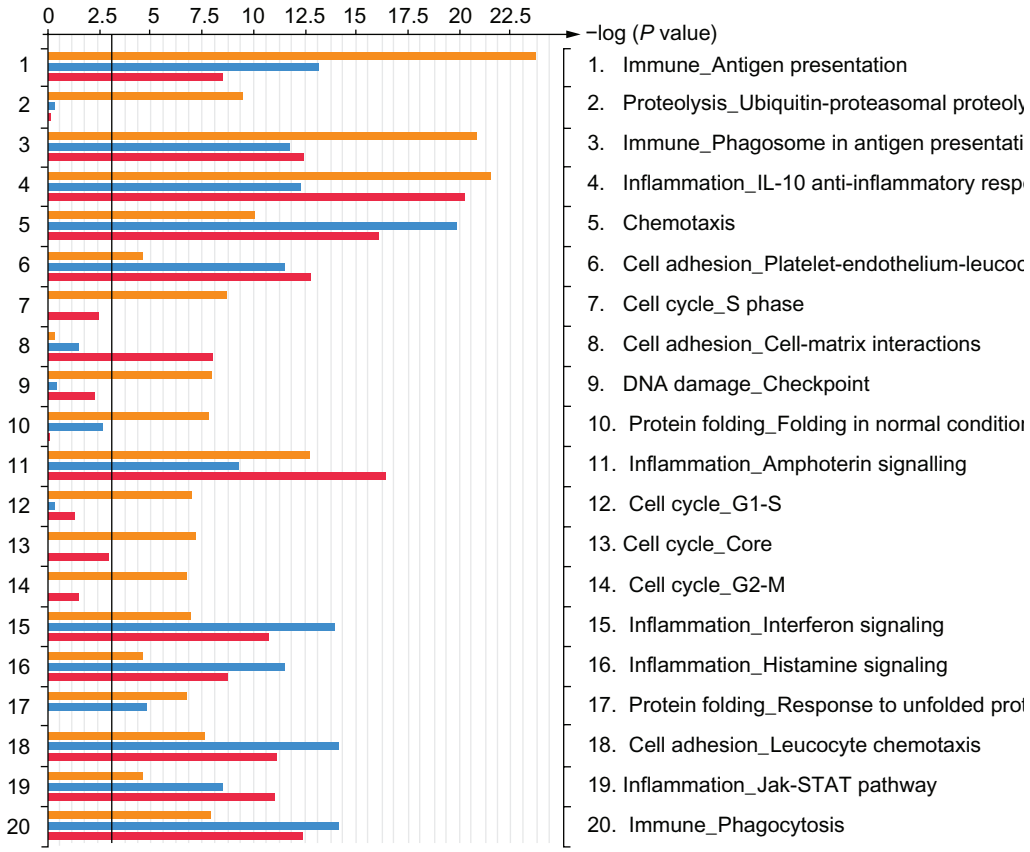

Figure 3. Results of GeneGo mapping of differentially affected networks. The core genes from significantly altered gene sets associated with each DEP/OVA exposure (N-DEP/OVA-blue; A-DEP/OVA-red; C-DEP/OVA-orange) was imported into GeneGo to generate a list of the top 20 networks.

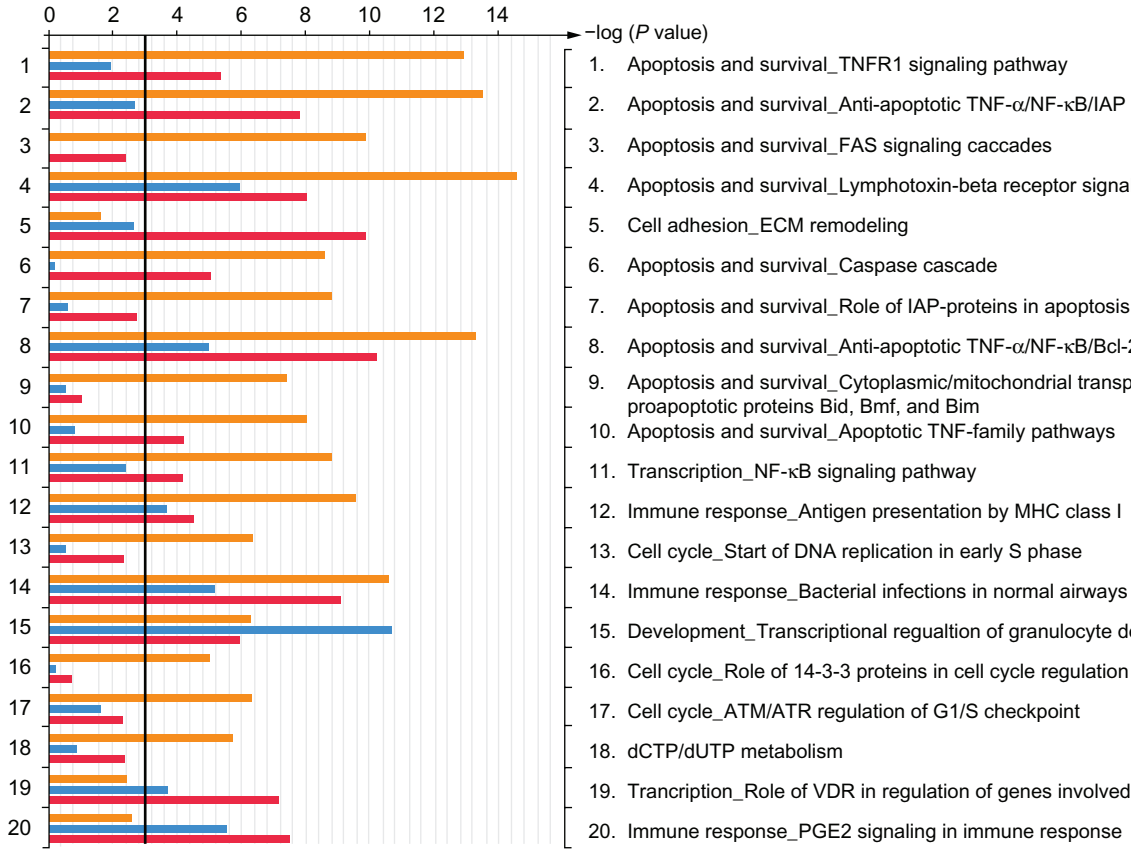

Figure 4. Results of GeneGo mapping of differentially affected pathways. The core genes from significantly altered gene sets associated with each DEP/OVA exposure (N-DEP/OVA-blue; A-DEP/OVA-red; C-DEP/OVA-orange) was imported into GeneGo to generate a list of the top 20 pathways.

A- and C-DEP/OVA samples altered apoptosis pathways while the most biologically active DEP sample, C-DEP/OVA, also altered cell cycle and DNA repair networks.

We recently reported the inflammatory and adjuvant effects of the above three diesels, N-, A-, and C-DEP.[11] Although it is important to identify individual genes associated with adverse biological effects, the resulting phenotypic changes likely occur through interactions of multiple genes. Therefore, to associate transcriptional responses with the allergic phenotype we utilized a global approach to a) characterize the genomic signature of DEP as a class and b) identify pathways common and unique to the DEP/OVA exposures.

Our genomic signature response to DEP as a class compound is well supported by the literature. DEP exposure has been shown to induce lung inflammation as manifested by neutrophil infiltration and elevated levels of total protein, albumin, LDH, and reactive oxygen species (ROS) in the lung as well as up-regulation of inflammatory cytokines.[3,11,12,19,20] Furthermore, DEP and other particles including ambient PM have been shown to induce TLR4 expression in the lung,[21,22] while TLR4 deficient mice developed less airway inflammation in response to DEP compared to wild type controls.[23] In agreement with these findings, our results demonstrated the cytokine-cytokine receptor and the TLR interaction KEGG pathways were significantly altered in all DEP/saline exposures. These findings not only provide further evidence for the TLR pathway involvement in DEP induced inflammatory response, but also confirmed a common genomic signature response of DEP, regardless of chemical composition.

It has been established that while DEP alone can induce an inflammatory response, when given with an antigen they also act as an immunologic adjuvant.[3–6] The DEP/OVA exposures did not alter KEGG pathways such as antigen processing and presentation or T cell receptor signaling. Instead, in a similar fashion to DEP alone, genomic analysis of all the DEP/OVA exposed samples displayed common alterations in the cytokine-cytokine receptor and TLR KEGG pathways.

This is a likely response because under this analysis all DEP/OVA samples were compared to OVA exposure. However, compared to DEP/saline, DEP/OVA exposed samples showed a more pronounced increase in the number of genes enriched in these pathways. This provides further evidence, on the genomic level, that DEP and OVA interacted synergistically to produce an immuno-modulatory effect.

Li et al[24] proposed a hierarchical oxidative stress model to explain DEP induced effects whereby low levels of oxidative stress induce antioxidant defense mechanisms to restore redox balance in the cell (tier 1). Intermediate levels of oxidative stress (tier 2) activate MAPK and NF-κB cascades, which induce inflammation, while high levels of oxidative stress (tier 3) activate apoptosis and apoptosis/necrosis pathways.[24] In agreement with this model, the study presented here demonstrates similar effects *in vivo*. Antioxidant transcription factors and enzymes such as Nrf2, heme oxygenase 1 (HO-1), and superoxide dismutase 2 (SOD2) were up-regulated in response to all three DEP/OVA exposures, indicative of low levels of oxidative stress (tier 1). The tier 2 responses, MAPKs, NF-κB, as well as inflammatory, T_H1, and T_H2 cytokines and chemokines, were also up-regulated in all three DEP/OVA exposures. In addition, A- and C-DEP/OVA exposures altered apoptosis (tier 3) pathways with C-DEP/OVA having altered the greatest number of these pathways. From this analysis it would appear that these early changes were predictive of the previously reported post-challenge phenotype.[11]

It has been established that DEP organic compounds can generate ROS[25] and excessive ROS production can lead to a variety of cellular responses including DNA damage.[26] In fact, oxidative DNA damage (8-hydroxydeoxyguanosine) has been detected in mouse lung DNA after DEP exposure.[27] Although the A-DEP sample contained the greatest amount of DCM EOM, C-DEP contained the greatest amount of PAHs[11] and the C-DEP/OVA exposure group was unique in significantly altering cell cycle and DNA damage pathways. Global transcriptional analysis of lung tissue revealed up-regulation of cell cycle control genes including 6 cyclin genes, 7 cell division cycle genes, 7 members of the family of MAP kinases, 2 cyclin-dependent kinases, RAS p21 protein activator 3 (Rasa3), and 5 other RAS related proteins. Although we can not say with certainty that these changes were due to the PAH content, this evidence suggests the newer C-DEP sample generated more oxidative damage.

Conclusion

In conclusion, mice exposed to all three DEP samples with or without OVA had altered cytokine and toll-like receptor pathways suggesting these responses are common to all DEPs regardless of chemical profile. All DEP/OVA exposures increased transcription of genes involved in tier 1 and 2 of the hierarchical stress response model described by Li et al.[24,28,29] Additionally, A- and C-DEP/OVA exposures significantly altered the most number of apoptosis pathways (tier 3). The C-DEP/OVA also altered cell cycle and DNA damage pathways suggesting it is the most bioactive sample. While the C-DEP sample also contained the largest amount of PAHs, these studies were not designed to address whether these components were causal to the effect. Nevertheless, it is known that PAHs can induce a pro-allergic effect.[30–32] This comprehensive approach using gene expression analysis to examine pathway changes at a transcriptional level provides a clearer picture of the events occurring in the lung after DEP exposure in the presence or absence of antigen. The results illustrate a wide range of altered pathways suggesting this method may be more sensitive and can be used for identifying mechanisms involved in induction of immune responses that lead to increased severity of allergic lung disease.

Funding

The project described was supported by the EPA-UNC Curriculum in Toxicology Training agreement (# T829472). This paper has been reviewed by the National Health and Environmental Effects Research Laboratory, U.S. Environmental Protection Agency, and approved for publication. Approval does not signify that the contents necessarily reflect the views and policies of the Agency, nor does the mention of trade names or commercial products constitute endorsement or recommendation for use.

Acknowledgements

Dr. William Ward for review of the manuscript and helpful suggestions.

Disclosures

This manuscript has been read and approved by all authors. This paper is unique and is not under consideration by any other publication and has not been published elsewhere. The authors and peer reviewers of this paper report no conflicts of interest. The authors confirm that they have permission to reproduce any copyrighted material.

References

1. Sydbom A, et al. Health effects of diesel exhaust emissions. *Eur Respir J*. 2001;17(4):733–46.
2. Schuetzle D. Sampling of vehicle emissions for chemical analysis and biological testing. *Environ Health Perspect*. 1983;47:65–80.
3. Bayram H, et al. The effect of diesel exhaust particles on cell function and release of inflammatory mediators from human bronchial epithelial cells in vitro. *Am J Respir Cell Mol Biol*. 1998;18(3):441–8.
4. Diaz-Sanchez D, et al. Enhanced nasal cytokine production in human beings after in vivo challenge with diesel exhaust particles. *J Allergy Clin Immunol*. 1996;98(1):114–23.
5. Steerenberg PA, et al. Adjuvant activity of various diesel exhaust and ambient particle in two allergic models. *J Toxicol Environ Health A*. 2003;66(15):1421–39.
6. Takafuji S, et al. Diesel-exhaust particulates inoculated by the intranasal route have an adjuvant activity for IgE production in mice. *J Allergy Clin Immunol*. 1987;79(4):639–45.
7. Yanagisawa R, et al. Components of diesel exhaust particles differentially affect Th1/Th2 response in a murine model of allergic airway inflammation. *Clin Exp Allergy*. 2006;36(3):386–95.
8. Singh P, et al. Sample characterization of automobile and forklift diesel exhaust particles and comparative pulmonary toxicity in mice. *Environ Health Perspect*. 2004;112(8):820–5.
9. Ohtani T, et al. Cellular basis of the role of diesel exhaust particles in inducing Th2-dominant response. *J Immunol*. 2005;174(4):2412–9.
10. Ma JY, Ma JK. The dual effect of the particulate and organic components of diesel exhaust particles on the alteration of pulmonary immune/inflammatory responses and metabolic enzymes. *J Environ Sci Health C Environ Carcinog Ecotoxicol Rev*. 2002;20(2):117–47.
11. Stevens T, et al. Differential potentiation of allergic lung disease in mice exposed to chemically distinct diesel samples. *Toxicol Sci*. 2009;107(2): 522–34.
12. Stevens T, et al. Increased transcription of immune and metabolic pathways in naive and allergic mice exposed to diesel exhaust. *Toxicol Sci*. 2008;102(2):359–70.
13. Kobayashi T, Ito T. Diesel exhaust particulates induce nasal mucosal hyperresponsiveness to inhaled histamine aerosol. *Fundam Appl Toxicol*. 1995;27(2):195–202.
14. Sagai M, et al. Biological effects of diesel exhaust particles. I. In vitro production of superoxide and in vivo toxicity in mouse. *Free Radic Biol Med*. 1993;14(1):37–47.
15. Cao D, et al. Diesel exhaust particulate-induced activation of Stat3 requires activities of EGFR and Src in airway epithelial cells. *Am J Physiol Lung Cell Mol Physiol*. 2007;292(2):L422–9.
16. Irizarry RA, et al. Exploration, normalization, and summaries of high density oligonucleotide array probe level data. *Biostatistics*. 2003;4(2):249–64.
17. Subramanian A, et al. Gene set enrichment analysis: a knowledge-based approach for interpreting genome-wide expression profiles. *Proc Natl Acad Sci U S A*. 2005;102(43):15545–50.
18. Bild A, Febbo PG. Application of a priori established gene sets to discover biologically important differential expression in microarray data. *Proc Natl Acad Sci U S A*. 2005;102(43):15278–9.
19. Ito T, et al. Peroxynitrite formation by diesel exhaust particles in alveolar cells: Links to pulmonary inflammation. *Environ Toxicol Pharmacol*. 2000;9(1–2):1–8.
20. Singh P, et al. Sample Characterization of Automobile and Forklift Diesel Exhaust Particles and Comparative Pulmonary Toxicity in Mice. *Environ Health Perspect*. 2004;112(8):820–5.
21. Takano H, et al. Diesel exhaust particles enhance lung injury related to bacterial endotoxin through expression of proinflammatory cytokines, chemokines, and intercellular adhesion molecule-1. *Am J Respir Crit Care Med*. 2002;165(9):1329–35.
22. Williams MA, et al. TLR2 and TLR4 as Potential Biomarkers of Environmental Particulate Matter Exposed Human Myeloid Dendritic Cells. *Biomark Insights*. 2007;2:226–40.
23. Inoue K, et al. The role of toll-like receptor 4 in airway inflammation induced by diesel exhaust particles. *Arch Toxicol*. 2006;80(5):275–9.
24. Li N, et al. Particulate air pollutants and asthma. A paradigm for the role of oxidative stress in PM-induced adverse health effects. *Clin Immunol*. 2003;109(3):250–65.
25. Casillas AM, et al. Enhancement of allergic inflammation by diesel exhaust particles: permissive role of reactive oxygen species. *Ann Allergy Asthma Immunol*. 1999;83(6 Pt 2):624–9.
26. Risom L, Moller P, Loft S. Oxidative stress-induced DNA damage by particulate air pollution. *Mutat Res*. 2005;592(1–2):119–37.
27. Nagashima M, et al. Formation of an oxidative DNA damage, 8-hydroxydeoxyguanosine, in mouse lung DNA after intratracheal instillation of diesel exhaust particles and effects of high dietary fat and beta-carotene on this process. *Carcinogenesis*. 1995;16(6):1441–5.
28. Li N, et al. Use of a stratiefied oxidative stress model to study the biological effects of ambient concentrated and diesel exhaust particulate matter. *Inhalation Toxicology*. 2002;14:459–86.
29. Li N, et al. Ultrafine particulate pollutants induce oxidative stress and mitochondrial damage. *Environ Health Perspect*. 2003;111(4):455–60.
30. Schober W, et al. Environmental polycyclic aromatic hydrocarbons (PAHs) enhance allergic inflammation by acting on human basophils. *Inhal Toxicol*. 2007;19 Suppl 1:151–6.
31. Lubitz S, et al. Polycyclic aromatic hydrocarbons from diesel emissions exert proallergic effects in birch pollen allergic individuals through enhanced mediator release from basophils. *Environ Toxicol*. 2009.
32. Kepley CL, et al. Environmental polycyclic aromatic hydrocarbons, benzo(a) pyrene (BaP) and BaP-quinones, enhance IgE-mediated histamine release and IL-4 production in human basophils. *Clin Immunol*. 2003;107(1):10–9.

Appendix

Appendix 1. Significantly altered gene sets by N-DEP/saline compared to saline.

Name	Sise	ES	NES	FDR q-val
CARIES_PULP_HIGH_UP	68	0.81	2.85	<1.00E-06
LAL_KO_3MO_UP	46	0.84	2.80	<1.00E-06
FLECHNER_KIDNEY_TRANSPLANT_ REJECTION_UP	72	0.78	2.79	<1.00E-06
LINDSTEDT_DEND_8H_VS_48H_UP	58	0.81	2.78	<1.00E-06
LAL_KO_6MO_UP	58	0.80	2.75	<1.00E-06
WIELAND_HEPATITIS_B_INDUCED	71	0.77	2.71	<1.00E-06
GALINDO_ACT_UP	75	0.74	2.66	<1.00E-06
YANG_OSTECLASTS_SIG	39	0.84	2.61	<1.00E-06
NAKAJIMA_MCS_UP	85	0.70	2.55	<1.00E-06
BLEO_HUMAN_LYMPH_HIGH_24HRS_UP	86	0.69	2.54	<1.00E-06
BASSO_GERMINAL_CENTER_CD40_UP	82	0.69	2.54	<1.00E-06
HINATA_NFKB_UP	89	0.69	2.52	<1.00E-06
NADLER_OBESITY_UP	57	0.73	2.51	<1.00E-06
SANA_TNFA_ENDOTHELIAL_UP	61	0.72	2.50	<1.00E-06
NEMETH_TNF_UP	82	0.69	2.49	<1.00E-06
MUNSHI_MM_VS_PCS_UP	64	0.67	2.34	<1.00E-06
MUNSHI_MM_UP	57	0.69	2.34	7.18E-05
NI2_MOUSE_UP	40	0.74	2.33	6.78E-05
TNFA_NFKB_DEP_UP	17	0.86	2.33	6.43E-05
SHIPP_FL_VS_DLBCL_DN	30	0.74	2.24	6.11E-05
LINDSTEDT_DEND_UP	44	0.69	2.23	5.81E-05
TAVOR_CEBP_UP	42	0.69	2.22	5.55E-05
HOUSTIS_ROS	32	0.73	2.21	5.31E-05
MARTINELLI_IFNS_DIFF	16	0.83	2.19	5.09E-05
ZUCCHI_EPITHELIAL_DN	36	0.68	2.19	4.88E-05
TPA_SENS_MIDDLE_UP	55	0.64	2.17	1.39E-04
ROSS_CBF_MYH	38	0.70	2.17	2.21E-04
CROONQUIST_IL6_RAS_UP	18	0.81	2.15	2.99E-04
ZHAN_MULTIPLE_MYELOMA_VS_ NORMAL_DN	33	0.71	2.15	2.89E-04
NAKAJIMA_MCSMBP_MAST	37	0.69	2.14	3.19E-04
ABBUD_LIF_UP	45	0.66	2.14	3.09E-04
KNUDSEN_PMNS_UP	65	0.62	2.14	2.99E-04
JECHLINGER_EMT_UP	56	0.63	2.12	4.73E-04
DAC_BLADDER_UP	23	0.76	2.12	4.59E-04
DAC_IFN_BLADDER_UP	16	0.82	2.12	4.46E-04
PEART_HISTONE_DN	63	0.61	2.11	4.34E-04
RADAEVA_IFNA_UP	38	0.67	2.10	4.22E-04
ZELLER_MYC_UP	23	0.73	2.10	4.11E-04
CANCER_UNDIFFERENTIATED_META_ UP	62	0.61	2.10	4.62E-04
MARSHALL_SPLEEN_BAL	25	0.74	2.09	4.50E-04
PROTEASOMEPATHWAY	21	0.73	2.09	4.69E-04
TNFALPHA_ALL_UP	66	0.59	2.08	5.41E-04
EMT_UP	55	0.60	2.08	5.29E-04
SCHUMACHER_MYC_UP	47	0.63	2.07	5.17E-04
PASSERINI_INFLAMMATION	23	0.73	2.07	5.05E-04
APPEL_IMATINIB_UP	29	0.70	2.07	4.94E-04
MYC_TARGETS	39	0.65	2.07	4.84E-04
ADIP_DIFF_CLUSTER4	31	0.68	2.07	4.99E-04
CMV_24HRS_UP	61	0.61	2.06	4.89E-04
OXIDATIVE_PHOSPHORYLATION	55	0.61	2.06	5.28E-04
CMV_ALL_UP	81	0.57	2.05	6.36E-04

(*Continued*)

Appendix 1. (*Continued*)

Name	Size	ES	NES	FDR q-val
HOFMANN_MDS_CD34_LOW_AND_ HIGH_RISK	31	0.68	2.05	7.14E-04
FERRANDO_MLL_T_ALL_DN	71	0.57	2.03	9.73E-04
IFNALPHA_NL_UP	19	0.74	2.01	1.16E-03
ERM_KO_SERTOLI_DN	17	0.77	2.01	1.18E-03
AGED_MOUSE_NEOCORTEX_UP	60	0.59	2.01	1.16E-03
INOS_ALL_UP	47	0.61	2.01	1.16E-03
CANTHARIDIN_DN	45	0.61	2.00	1.22E-03
COLLER_MYC_UP	17	0.77	2.00	1.43E-03
ROS_MOUSE_AORTA_DN	68	0.57	2.00	1.40E-03
PROTEASOME	17	0.75	2.00	1.38E-03
NKTPATHWAY	28	0.67	1.99	1.53E-03
HADDAD_CD45CD7_PLUS_VS_MINUS_ UP	52	0.58	1.99	1.51E-03
IL6_FIBRO_UP	35	0.63	1.99	1.48E-03
HEARTFAILURE_VENTRICLE_DN	56	0.59	1.99	1.55E-03
APOPTOSIS	64	0.56	1.98	1.84E-03
TAKEDA_NUP8_HOXA9_3D_DN	20	0.71	1.97	1.85E-03
LIAN_MYELOID_DIFF_GRANULE	28	0.67	1.96	2.33E-03
HADDAD_HSC_CD7_UP	52	0.58	1.96	2.39E-03
ST_TUMOR_NECROSIS_FACTOR_ PATHWAY	28	0.67	1.96	2.56E-03
MOOTHA_VOXPHOS	73	0.55	1.95	2.71E-03
CHAUHAN_2ME2	42	0.60	1.95	2.76E-03
RIBOSOMAL_PROTEINS	78	0.54	1.95	2.77E-03
TNFALPHA_4HRS_UP	34	0.63	1.94	2.91E-03
LEE_MYC_TGFA_UP	54	0.57	1.94	2.89E-03
MOREAUX_TACI_HI_IN_PPC_UP	43	0.59	1.94	2.97E-03
BHATTACHARYA_ESC_UP	57	0.57	1.94	3.07E-03
BRCA_BRCA1_POS	68	0.56	1.94	3.09E-03
IFNALPHA_HCC_UP	23	0.70	1.94	3.13E-03
DSRNA_UP	32	0.64	1.94	3.09E-03
PROTEASOME_DEGRADATION	32	0.64	1.93	3.26E-03
BENNETT_SLE_UP	19	0.70	1.93	3.39E-03
TARTE_PC	65	0.55	1.93	3.58E-03
CMV_HCMV_TIMECOURSE_12HRS_ UP	21	0.69	1.93	3.58E-03
TNFALPHA_30MIN_UP	37	0.61	1.92	3.71E-03
UVB_NHEK3_C0	73	0.54	1.92	3.89E-03
GOLDRATH_CYTOLYTIC	24	0.67	1.92	3.84E-03
LIAN_MYELOID_DIFF_RECEPTORS	33	0.61	1.92	3.84E-03
PARK_RARALPHA_UP	34	0.61	1.91	4.34E-03
IL2PATHWAY	21	0.68	1.90	4.71E-03
STEMCELL_COMMON_DN	54	0.56	1.90	4.66E-03
AGED_MOUSE_CEREBELLUM_UP	58	0.55	1.89	5.69E-03
DER_IFNG_UP	54	0.56	1.88	6.10E-03
CCR5PATHWAY	18	0.70	1.87	7.21E-03
HALMOS_CEBP_UP	41	0.57	1.86	8.29E-03
ZHAN_MM_CD138_MF_VS_REST	30	0.62	1.85	8.56E-03
HOHENKIRK_MONOCYTE_DEND_ UP	85	0.51	1.85	8.52E-03
ST_GAQ_PATHWAY	24	0.65	1.85	8.95E-03
PHOTOSYNTHESIS	21	0.67	1.85	9.02E-03
IFN_GAMMA_UP	35	0.59	1.84	9.97E-03
IFNA_UV-CMV_COMMON_HCMV_6HRS_ UP	20	0.67	1.84	9.88E-03

Abbreviations: ES, enrichment score; NES, normalized enrichment score; FDR, false discovery rate.

Appendix 2. Significantly altered gene sets by A-DEP/saline compared to saline.

Name	Size	ES	NES	FDR q-val
CARIES_PULP_HIGH_UP	68	0.77	2.89	<1.00E-06
LAL_KO_3MO_UP	46	0.78	2.73	<1.00E-06
LAL_KO_6MO_UP	58	0.73	2.65	<1.00E-06
DNA_REPLICATION_REACTOME	41	0.75	2.55	<1.00E-06
ELECTRON_TRANSPORT_CHAIN	86	0.65	2.55	<1.00E-06
CANCER_UNDIFFERENTIATED_META_UP	62	0.69	2.51	<1.00E-06
MOOTHA_VOXPHOS	73	0.67	2.48	<1.00E-06
YANG_OSTECLASTS_SIG	39	0.74	2.45	<1.00E-06
MANALO_HYPOXIA_DN	73	0.65	2.44	<1.00E-06
CANCER_NEOPLASTIC_META_UP	59	0.68	2.44	<1.00E-06
YU_CMYC_UP	37	0.72	2.38	<1.00E-06
GALINDO_ACT_UP	75	0.62	2.37	<1.00E-06
OXIDATIVE_PHOSPHORYLATION	55	0.66	2.36	<1.00E-06
FLECHNER_KIDNEY_TRANSPLANT_ REJECTION_UP	72	0.62	2.34	<1.00E-06
LINDSTEDT_DEND_8H_VS_48H_UP	58	0.65	2.32	<1.00E-06
CANTHARIDIN_DN	45	0.66	2.31	<1.00E-06
SERUM_FIBROBLAST_CELLCYCLE	88	0.58	2.30	<1.00E-06
FERRANDO_MLL_T_ALL_DN	71	0.61	2.30	<1.00E-06
SCHUMACHER_MYC_UP	47	0.66	2.29	<1.00E-06
WIELAND_HEPATITIS_B_INDUCED	71	0.62	2.29	<1.00E-06
ADIP_DIFF_CLUSTER4	31	0.72	2.28	<1.00E-06
P21_ANY_DN	27	0.74	2.28	<1.00E-06
HOUSTIS_ROS	32	0.71	2.27	<1.00E-06
PEART_HISTONE_DN	63	0.62	2.27	<1.00E-06
IDX_TSA_UP_CLUSTER3	81	0.60	2.26	4.59E-05
NEMETH_TNF_UP	82	0.59	2.25	4.42E-05
CMV_IE86_UP	42	0.67	2.24	4.25E-05
BLEO_HUMAN_LYMPH_HIGH_24HRS_UP	86	0.57	2.21	4.10E-05
INOS_ALL_UP	47	0.64	2.21	3.96E-05
MENSSEN_MYC_UP	30	0.70	2.21	3.83E-05
UVB_NHEK2_UP	55	0.61	2.17	2.29E-04
NI2_MOUSE_UP	40	0.64	2.16	2.97E-04
PROTEASOME_DEGRADATION	32	0.67	2.15	4.35E-04
RIBOSOMAL_PROTEINS	78	0.56	2.15	4.57E-04
BHATTACHARYA_ESC_UP	57	0.59	2.12	5.44E-04
HG_PROGERIA_DN	24	0.71	2.12	5.29E-04
NAKAJIMA_MCS_UP	85	0.55	2.12	5.47E-04
COLLER_MYC_UP	17	0.76	2.10	6.62E-04
HEARTFAILURE_VENTRICLE_DN	56	0.58	2.09	6.74E-04
OLDAGE_DN	45	0.61	2.09	6.58E-04
BASSO_GERMINAL_CENTER_CD40_UP	82	0.54	2.07	9.37E-04
DOX_RESIST_GASTRIC_UP	30	0.65	2.06	1.26E-03
ZELLER_MYC_UP	23	0.69	2.04	1.70E-03
UVB_NHEK1_C1	41	0.60	2.03	1.69E-03
MOREAUX_TACI_HI_IN_PPC_UP	43	0.60	2.03	1.70E-03
RIBAVIRIN_RSV_UP	18	0.72	2.01	2.22E-03
P21_P53_ANY_DN	35	0.62	2.01	2.17E-03
BREAST_DUCTAL_CARCINOMA_GENES	19	0.71	2.01	2.30E-03
CMV_24HRS_UP	61	0.55	2.00	2.42E-03
REN_E2F1_TARGETS	37	0.60	2.00	2.52E-03

(Continued)

(*Continued*)

Appendix 2. (*Continued*)

Name	Size	ES	NES	FDR q-val
IDX_TSA_UP_CLUSTER5	82	0.52	2.00	2.49E-03
CROONQUIST_IL6_STARVE_UP	32	0.62	1.99	2.51E-03
TNFALPHA_ALL_UP	66	0.53	1.99	2.60E-03
TSA_CD4_UP	24	0.65	1.99	2.55E-03
PYRIMIDINE_METABOLISM	55	0.55	1.98	2.90E-03
HINATA_NFKB_UP	89	0.51	1.97	3.15E-03
MYC_TARGETS	39	0.59	1.96	3.66E-03
ADIP_DIFF_CLUSTER5	34	0.59	1.95	4.09E-03
SHIPP_FL_VS_DLBCL_DN	30	0.61	1.95	4.06E-03
TNFA_NFKB_DEP_UP	17	0.71	1.95	4.23E-03
ATP_SYNTHESIS	20	0.67	1.95	4.18E-03
TNFALPHA_30MIN_UP	37	0.58	1.95	4.12E-03
HPV31_DN	37	0.58	1.94	4.28E-03
P21_P53_MIDDLE_DN	17	0.71	1.94	4.23E-03
TAVOR_CEBP_UP	42	0.57	1.93	4.64E-03
PHOTOSYNTHESIS	21	0.67	1.93	4.74E-03
PROTEASOMEPATHWAY	21	0.65	1.92	5.43E-03
TARTE_PC	65	0.52	1.91	5.70E-03
TYPE_III_SECRETION_SYSTEM	20	0.67	1.91	5.66E-03
CMV_ALL_UP	81	0.50	1.91	5.88E-03
UEDA_MOUSE_SCN	86	0.49	1.91	5.82E-03
G1_TO_S_CELL_CYCLE_REACTOME	65	0.51	1.90	6.40E-03
STRESS_TPA_SPECIFIC_UP	34	0.59	1.90	6.36E-03
CELL_CYCLE	71	0.50	1.90	6.42E-03
FLAGELLAR_ASSEMBLY	20	0.67	1.89	6.60E-03
ABBUD_LIF_UP	45	0.54	1.89	7.01E-03
KNUDSEN_PMNS_UP	65	0.51	1.88	7.46E-03
TPA_SENS_MIDDLE_UP	55	0.53	1.88	7.62E-03
CARBON_FIXATION	18	0.66	1.88	7.67E-03
MMS_HUMAN_LYMPH_HIGH_24HRS_UP	18	0.69	1.88	7.58E-03
ZHAN_MM_CD138_PR_VS_REST	28	0.62	1.87	7.97E-03
ZUCCHI_EPITHELIAL_DN	36	0.58	1.87	8.21E-03
TIS7_OVEREXP_DN	17	0.67	1.87	8.23E-03
ZHAN_MULTIPLE_MYELOMA_VS_ NORMAL_DN	33	0.58	1.87	8.23E-03
ROS_MOUSE_AORTA_DN	68	0.50	1.87	8.17E-03
BRENTANI_DNA_METHYLATION_AND_ MODIFICATION	23	0.63	1.86	8.83E-03
NADLER_OBESITY_UP	57	0.52	1.86	8.73E-03
BLEO_MOUSE_LYMPH_LOW_24HRS_DN	24	0.63	1.86	8.70E-03
ET743_SARCOMA_UP	56	0.51	1.86	8.63E-03
UVB_NHEK3_C6	25	0.61	1.85	9.32E-03

Abbreviations: ES, enrichment score; NES, normalized enrichment score; FDR, false discovery rate.

Appendix 3. Significantly altered gene sets by C-DEP/saline compared to saline.

Name	Size	ES	NES	FDR q-val
CARIES_PULP_HIGH_UP	68	0.77	2.90	<1.00E-06
GALINDO_ACT_UP	75	0.72	2.79	<1.00E-06
YANG_OSTECLASTS_SIG	39	0.79	2.74	<1.00E-06
LINDSTEDT_DEND_8H_VS_48H_UP	58	0.70	2.69	<1.00E-06
HINATA_NFKB_UP	89	0.65	2.64	<1.00E-06
NAKAJIMA_MCS_UP	85	0.65	2.58	<1.00E-06
NEMETH_TNF_UP	82	0.64	2.57	<1.00E-06
LAL_KO_6MO_UP	58	0.68	2.57	<1.00E-06
WIELAND_HEPATITIS_B_INDUCED	71	0.66	2.53	<1.00E-06
LAL_KO_3MO_UP	46	0.73	2.52	<1.00E-06
HOUSTIS_ROS	32	0.75	2.49	<1.00E-06
SANA_TNFA_ENDOTHELIAL_UP	61	0.66	2.48	<1.00E-06
FLECHNER_KIDNEY_TRANSPLANT_ REJECTION_UP	72	0.64	2.47	<1.00E-06
BLEO_HUMAN_LYMPH_HIGH_24HRS_UP	86	0.61	2.45	<1.00E-06
NADLER_OBESITY_UP	57	0.66	2.45	<1.00E-06
ADIP_DIFF_CLUSTER4	31	0.74	2.44	<1.00E-06
MYC_TARGETS	39	0.71	2.44	<1.00E-06
TNFA_NFKB_DEP_UP	17	0.86	2.42	<1.00E-06
NI2_MOUSE_UP	40	0.71	2.41	<1.00E-06
INOS_ALL_UP	47	0.68	2.39	<1.00E-06
TPA_SENS_MIDDLE_UP	55	0.66	2.38	<1.00E-06
TSA_CD4_UP	24	0.76	2.35	<1.00E-06
CANCER_UNDIFFERENTIATED_META_UP	62	0.62	2.35	<1.00E-06
ZELLER_MYC_UP	23	0.76	2.33	<1.00E-06
ZUCCHI_EPITHELIAL_DN	36	0.70	2.33	<1.00E-06
CMV_IE86_UP	42	0.66	2.26	5.58E-05
CMV_24HRS_UP	61	0.59	2.26	5.37E-05
MUNSHI_MM_UP	57	0.59	2.24	1.03E-04
DAC_BLADDER_UP	23	0.74	2.23	1.47E-04
PASSERINI_INFLAMMATION	23	0.71	2.19	3.21E-04
BASSO_GERMINAL_CENTER_CD40_UP	82	0.56	2.19	3.11E-04
IDX_TSA_UP_CLUSTER3	81	0.56	2.18	4.32E-04
MARTINELLI_IFNS_DIFF	16	0.79	2.18	4.19E-04
CMV_ALL_UP	81	0.54	2.17	4.47E-04
P21_ANY_DN	27	0.69	2.16	4.73E-04
MANALO_HYPOXIA_DN	73	0.55	2.16	4.97E-04
MUNSHI_MM_VS_PCS_UP	64	0.58	2.15	5.20E-04
FERRANDO_MLL_T_ALL_DN	71	0.56	2.15	5.06E-04
SHIPP_FL_VS_DLBCL_DN	30	0.66	2.14	5.30E-04
MMS_HUMAN_LYMPH_HIGH_24HRS_UP	18	0.76	2.14	5.16E-04
DAC_IFN_BLADDER_UP	16	0.78	2.14	5.37E-04
DNA_REPLICATION_REACTOME	41	0.62	2.13	5.24E-04
PROTEASOME_DEGRADATION	32	0.66	2.13	5.43E-04
ROSS_CBF_MYH	38	0.61	2.12	7.18E-04
HG_PROGERIA_DN	24	0.70	2.11	7.33E-04
ROS_MOUSE_AORTA_DN	68	0.55	2.10	8.96E-04
OLDAGE_DN	45	0.60	2.09	1.05E-03
COLLER_MYC_UP	17	0.76	2.09	1.14E-03
KNUDSEN_PMNS_UP	65	0.55	2.08	1.29E-03
TARTE_PC	65	0.54	2.07	1.37E-03

(*Continued*)

Appendix 3. (*Continued*)

Name	Size	ES	NES	FDR q-val
PROTEASOME	17	0.75	2.07	1.37E-03
DER_IFNG_UP	54	0.56	2.06	1.37E-03
CANCER_NEOPLASTIC_META_UP	59	0.55	2.06	1.40E-03
CHAUHAN_2ME2	42	0.60	2.06	1.48E-03
SCHUMACHER_MYC_UP	47	0.60	2.06	1.45E-03
UVB_NHEK2_UP	55	0.57	2.06	1.50E-03
NKTPATHWAY	28	0.65	2.06	1.50E-03
MENSSEN_MYC_UP	30	0.64	2.06	1.52E-03
SERUM_FIBROBLAST_CELLCYCLE	88	0.52	2.05	1.54E-03
TAVOR_CEBP_UP	42	0.59	2.05	1.58E-03
PROTEASOMEPATHWAY	21	0.69	2.04	1.71E-03
IFNALPHA_NL_UP	19	0.71	2.04	1.68E-03
JECHLINGER_EMT_UP	56	0.55	2.04	1.70E-03
ABBUD_LIF_UP	45	0.59	2.04	1.76E-03
IL6_FIBRO_UP	35	0.60	2.03	1.79E-03
PEART_HISTONE_DN	63	0.53	2.02	2.33E-03
AS3_FIBRO_DN	26	0.65	2.01	2.34E-03
YU_CMYC_UP	37	0.59	2.01	2.34E-03
P21_P53_MIDDLE_DN	17	0.71	2.01	2.31E-03
STRESS_TPA_SPECIFIC_UP	34	0.61	2.01	2.40E-03
DSRNA_UP	32	0.60	2.00	2.60E-03
ERM_KO_SERTOLI_DN	17	0.71	1.99	2.64E-03
RADAEVA_IFNA_UP	38	0.59	1.99	2.73E-03
TNFALPHA_4HRS_UP	34	0.60	1.99	2.90E-03
CANTHARIDIN_DN	45	0.55	1.98	2.97E-03
IFN_GAMMA_UP	35	0.59	1.98	3.04E-03
HOFMANN_MDS_CD34_LOW_AND_ HIGH_RISK	31	0.61	1.97	3.31E-03
ADIP_DIFF_CLUSTER5	34	0.59	1.97	3.27E-03
TIS7_OVEREXP_DN	17	0.69	1.97	3.22E-03
LIAN_MYELOID_DIFF_RECEPTORS	33	0.59	1.97	3.36E-03
MARSHALL_SPLEEN_BAL	25	0.63	1.95	4.34E-03
NAKAJIMA_MCSMBP_MAST	37	0.58	1.94	4.80E-03
TAKEDA_NUP8_HOXA9_3D_DN	20	0.67	1.93	5.19E-03
PYRIMIDINE_METABOLISM	55	0.52	1.93	5.34E-03
TNFALPHA_ALL_UP	66	0.51	1.92	6.17E-03
CMV_HCMV_TIMECOURSE_12HRS_UP	21	0.65	1.92	6.12E-03
HEARTFAILURE_VENTRICLE_DN	56	0.52	1.92	6.14E-03
IFNALPHA_HCC_UP	23	0.64	1.91	6.44E-03
HYPOXIA_REVIEW	68	0.50	1.91	6.64E-03
LINDSTEDT_DEND_UP	44	0.54	1.91	6.87E-03
CROONQUIST_IL6_RAS_UP	18	0.67	1.90	7.79E-03
LEE_MYC_TGFA_UP	54	0.51	1.89	7.81E-03
EMT_UP	55	0.51	1.89	8.20E-03
LEE_ACOX1_UP	58	0.51	1.89	8.21E-03
BENNETT_SLE_UP	19	0.65	1.88	8.45E-03
ZHAN_MMPC_SIMAL	41	0.55	1.88	8.40E-03
P21_P53_ANY_DN	35	0.57	1.88	8.63E-03
BREAST_DUCTAL_CARCINOMA_ GENES	19	0.65	1.88	8.74E-03

Abbreviations: ES, enrichment score; NES, normalized enrichment score; FDR, false discovery rate.

Appendix 4. Significantly altered gene sets by N-DEP/OVA compared to OVA.

Name	Size	ES	NES	FDR q-val
CARIES_PULP_HIGH_UP	68	0.81	2.76	<1.00E-06
LAL_KO_3MO_UP	46	0.83	2.61	<1.00E-06
LAL_KO_6MO_UP	58	0.79	2.60	<1.00E-06
NEMETH_TNF_UP	82	0.74	2.59	<1.00E-06
WIELAND_HEPATITIS_B_INDUCED	71	0.74	2.54	<1.00E-06
NADLER_OBESITY_UP	57	0.76	2.51	<1.00E-06
YANG_OSTECLASTS_SIG	39	0.82	2.50	<1.00E-06
LINDSTEDT_DEND_8H_VS_48H_UP	58	0.73	2.45	<1.00E-06
NAKAJIMA_MCS_UP	85	0.69	2.44	<1.00E-06
SANA_TNFA_ENDOTHELIAL_UP	61	0.71	2.41	<1.00E-06
BASSO_GERMINAL_CENTER_CD40_UP	82	0.69	2.40	<1.00E-06
GALINDO_ACT_UP	75	0.69	2.40	<1.00E-06
FLECHNER_KIDNEY_TRANSPLANT_ REJECTION_UP	72	0.69	2.39	<1.00E-06
HINATA_NFKB_UP	89	0.64	2.26	<1.00E-06
NI2_MOUSE_UP	40	0.70	2.16	3.02E-04
BLEO_HUMAN_LYMPH_HIGH_24HRS_UP	86	0.60	2.14	2.83E-04
GOLDRATH_CYTOLYTIC	24	0.77	2.14	3.32E-04
BRENTANI_IMMUNE_FUNCTION	42	0.68	2.13	3.75E-04
JECHLINGER_EMT_UP	56	0.64	2.11	5.30E-04
ADIP_DIFF_CLUSTER3	28	0.73	2.10	5.03E-04
TNFA_NFKB_DEP_UP	17	0.80	2.09	5.83E-04
YU_CMYC_DN	53	0.65	2.09	5.57E-04
YAGI_AML_PROGNOSIS	31	0.70	2.07	7.26E-04
ROSS_MLL_FUSION	60	0.62	2.05	1.12E-03
LIAN_MYELOID_DIFF_RECEPTORS	33	0.69	2.03	1.47E-03
EMT_UP	55	0.61	2.02	1.50E-03
PASSERINI_INFLAMMATION	23	0.74	2.01	1.69E-03
APPEL_IMATINIB_UP	29	0.70	2.01	1.96E-03
ABBUD_LIF_UP	45	0.64	2.01	1.89E-03
TAKEDA_NUP8_HOXA9_3D_DN	20	0.74	2.01	1.86E-03
LINDSTEDT_DEND_DN	53	0.61	2.01	1.87E-03
CMV_ALL_UP	81	0.56	2.01	1.81E-03
TAVOR_CEBP_UP	42	0.63	1.99	2.34E-03
STEMCELL_COMMON_DN	54	0.60	1.98	2.89E-03
SCHUMACHER_MYC_UP	47	0.61	1.97	3.54E-03
ERM_KO_SERTOLI_DN	17	0.75	1.96	3.66E-03
DAC_IFN_BLADDER_UP	16	0.77	1.95	4.26E-03
SANA_IFNG_ENDOTHELIAL_UP	45	0.62	1.95	4.26E-03
WANG_HOXA9_VS_MEIS1_UP	25	0.68	1.94	4.75E-03
LIAN_MYELOID_DIFF_GRANULE	28	0.68	1.93	5.19E-03
CMV_24HRS_UP	61	0.58	1.93	5.58E-03
MARTINELLI_IFNS_DIFF	16	0.75	1.93	5.45E-03
TARTE_PC	65	0.56	1.92	5.48E-03
MYC_TARGETS	39	0.63	1.92	5.46E-03
WANG_MLL_CBP_VS_GMP_UP	42	0.61	1.91	6.10E-03
XU_CBP_UP	25	0.68	1.91	6.53E-03
LOTEM_LEUKEMIA_UP	22	0.69	1.91	6.39E-03
LINDSTEDT_DEND_UP	44	0.61	1.90	6.60E-03
LU_IL4BCELL	62	0.56	1.90	6.79E-03
ZELLER_MYC_UP	23	0.69	1.90	6.99E-03
CASPASEPATHWAY	20	0.69	1.90	6.89E-03
ROSS_CBF_MYH	38	0.62	1.90	6.76E-03

(*Continued*)

Appendix 4. (*Continued*)

Name	Size	ES	NES	FDR q-val
CMV_8HRS_UP	27	0.66	1.88	8.38E-03
TPA_SENS_MIDDLE_UP	55	0.57	1.88	8.27E-03
DSRNA_UP	32	0.63	1.87	8.52E-03
NAKAJIMA_MCSMBP_MAST	37	0.61	1.87	8.37E-03
CROONQUIST_IL6_RAS_UP	18	0.72	1.87	8.38E-03
GENOTOXINS_ALL_24HRS_REG	22	0.68	1.87	8.26E-03
HOHENKIRK_MONOCYTE_DEND_UP	85	0.53	1.87	8.40E-03
SHIPP_FL_VS_DLBCL_DN	30	0.63	1.87	8.34E-03

Abbreviations: ES, enrichment score; NES, normalized enrichment score; FDR, false discovery rate.

Appendix 5. Significantly altered gene sets by A-DEP/OVA compared to OVA.

Name	Size	ES	NES	FDR q-val
YANG_OSTECLASTS_SIG	39	0.86	2.84	<1.00E-06
LAL_KO_6MO_UP	58	0.74	2.59	<1.00E-06
NAKAJIMA_MCS_UP	85	0.68	2.58	<1.00E-06
LINDSTEDT_DEND_8H_VS_48H_UP	58	0.73	2.58	<1.00E-06
LAL_KO_3MO_UP	46	0.76	2.56	<1.00E-06
NADLER_OBESITY_UP	57	0.72	2.56	<1.00E-06
GALINDO_ACT_UP	75	0.70	2.54	<1.00E-06
SANA_TNFA_ENDOTHELIAL_UP	61	0.71	2.52	<1.00E-06
CARIES_PULP_HIGH_UP	68	0.70	2.50	<1.00E-06
NEMETH_TNF_UP	82	0.66	2.43	<1.00E-06
JECHLINGER_EMT_UP	56	0.67	2.32	<1.00E-06
HINATA_NFKB_UP	89	0.60	2.29	<1.00E-06
TNFA_NFKB_DEP_UP	17	0.85	2.29	<1.00E-06
NI2_MOUSE_UP	40	0.70	2.26	7.14E-05
ERM_KO_SERTOLI_DN	17	0.83	2.25	6.67E-05
BASSO_GERMINAL_CENTER_CD40_UP	82	0.61	2.24	6.25E-05
WIELAND_HEPATITIS_B_INDUCED	71	0.62	2.22	5.88E-05
EMT_UP	55	0.63	2.21	5.56E-05
PASSERINI_INFLAMMATION	23	0.75	2.19	5.26E-05
NAKAJIMA_MCSMBP_MAST	37	0.68	2.17	5.00E-05
TPA_SENS_MIDDLE_UP	55	0.62	2.16	4.76E-05
LIAN_MYELOID_DIFF_RECEPTORS	33	0.69	2.14	1.40E-04
BENNETT_SLE_UP	19	0.77	2.13	2.24E-04
TGFBETA_C2_UP	17	0.79	2.12	2.14E-04
TAKEDA_NUP8_HOXA9_3D_DN	20	0.76	2.12	2.48E-04
RADAEVA_IFNA_UP	38	0.65	2.10	3.19E-04
IL1_CORNEA_UP	53	0.60	2.08	5.72E-04
DAC_BLADDER_UP	23	0.72	2.08	5.89E-04
DAC_IFN_BLADDER_UP	16	0.79	2.08	6.03E-04
MARTINELLI_IFNS_DIFF	16	0.77	2.07	6.89E-04
TAVOR_CEBP_UP	42	0.62	2.06	7.32E-04
AS3_FIBRO_DN	26	0.70	2.05	7.74E-04
HEARTFAILURE_VENTRICLE_DN	56	0.59	2.03	1.03E-03
CANCER_UNDIFFERENTIATED_META_UP	62	0.56	2.01	1.43E-03
FLECHNER_KIDNEY_TRANSPLANT_ REJECTION_UP	72	0.55	2.01	1.39E-03
ADIP_DIFF_CLUSTER4	31	0.64	2.01	1.38E-03
KNUDSEN_PMNS_UP	65	0.56	2.00	1.39E-03

(*Continued*)

Appendix 5. (*Continued*)

Name	Size	ES	NES	FDR q-val
AGED_MOUSE_CEREBELLUM_UP	58	0.58	1.99	1.66E-03
CMV_ALL_UP	81	0.54	1.98	1.90E-03
BLEO_HUMAN_LYMPH_HIGH_24HRS_UP	86	0.52	1.98	2.06E-03
MATRIX_METALLOPROTEINASES	24	0.69	1.98	2.04E-03
DORSEY_DOXYCYCLINE_UP	23	0.68	1.96	2.53E-03
PASSERINI_EM	34	0.62	1.96	2.56E-03
TSA_CD4_UP	24	0.66	1.95	2.62E-03
CROONQUIST_IL6_RAS_UP	18	0.70	1.95	2.70E-03
ZUCCHI_EPITHELIAL_DN	36	0.60	1.94	3.52E-03
CMV_8HRS_UP	27	0.64	1.93	4.18E-03
IFNALPHA_HCC_UP	23	0.66	1.92	4.21E-03
SANA_IFNG_ENDOTHELIAL_UP	45	0.58	1.92	4.35E-03
APPEL_IMATINIB_UP	29	0.63	1.92	4.30E-03
SHEPARD_POS_REG_OF_CELL_ PROLIFERATION	85	0.52	1.92	4.22E-03
CROONQUIST_IL6_STROMA_UP	34	0.60	1.92	4.34E-03
SERUM_FIBROBLAST_CELLCYCLE	88	0.50	1.91	4.61E-03
DSRNA_UP	32	0.61	1.91	4.91E-03
MYC_TARGETS	39	0.58	1.90	5.89E-03
INSULIN_NIH3T3_UP	15	0.72	1.89	6.12E-03
CHAUHAN_2ME2	42	0.56	1.89	6.17E-03
CAMPTOTHECIN_PROBCELL_DN	21	0.66	1.89	6.08E-03
LINDSTEDT_DEND_DN	53	0.55	1.89	6.21E-03
LEE_DENA_UP	55	0.54	1.88	6.31E-03
ROSS_MLL_FUSION	60	0.53	1.88	6.51E-03
CCR5PATHWAY	18	0.68	1.88	6.64E-03
PEART_HISTONE_DN	63	0.52	1.88	6.61E-03
IRITANI_ADPROX_DN	45	0.55	1.87	7.03E-03
ABBUD_LIF_UP	45	0.56	1.87	7.16E-03
MUNSHI_MM_UP	57	0.53	1.87	7.10E-03
ZHAN_MULTIPLE_MYELOMA_VS_ NORMAL_DN	33	0.61	1.87	7.10E-03
NKTPATHWAY	28	0.62	1.85	9.28E-03

Abbreviations: ES, enrichment score; NES, normalized enrichment score; FDR, false discovery rate.

Appendix 6. Significantly altered gene sets by C-DEP/OVA compared to OVA.

Name	Size	ES	NES	FDR q-val
CARIES_PULP_HIGH_UP	68	0.80	2.94	<1.00E-06
WIELAND_HEPATITIS_B_INDUCED	71	0.76	2.83	<1.00E-06
NEMETH_TNF_UP	82	0.73	2.77	<1.00E-06
YANG_OSTECLASTS_SIG	39	0.82	2.73	<1.00E-06
LINDSTEDT_DEND_8H_VS_48H_UP	58	0.76	2.73	<1.00E-06
FLECHNER_KIDNEY_TRANSPLANT_ REJECTION_UP	72	0.73	2.71	<1.00E-06
IFNA_HCMV_6HRS_UP	38	0.80	2.64	<1.00E-06
LAL_KO_6MO_UP	58	0.76	2.64	<1.00E-06
GALINDO_ACT_UP	75	0.71	2.62	<1.00E-06
LAL_KO_3MO_UP	46	0.77	2.60	<1.00E-06
SANA_TNFA_ENDOTHELIAL_UP	61	0.73	2.59	<1.00E-06
CMV_ALL_UP	81	0.67	2.50	<1.00E-06
SANA_IFNG_ENDOTHELIAL_UP	45	0.74	2.50	<1.00E-06
RADAEVA_IFNA_UP	38	0.76	2.49	<1.00E-06
CMV_8HRS_UP	27	0.81	2.48	<1.00E-06

(*Continued*)

Appendix 6. (*Continued*)

Name	Size	ES	NES	FDR q-val
BASSO_GERMINAL_CENTER_CD40_UP	82	0.66	2.48	<1.00E-06
NAKAJIMA_MCS_UP	85	0.65	2.46	<1.00E-06
DER_IFNA_UP	53	0.69	2.45	<1.00E-06
CANCER_NEOPLASTIC_META_UP	59	0.69	2.45	<1.00E-06
DER_IFNB_UP	76	0.65	2.41	<1.00E-06
HINATA_NFKB_UP	89	0.63	2.41	<1.00E-06
CMV_HCMV_TIMECOURSE_12HRS_UP	21	0.82	2.39	<1.00E-06
CANCER_UNDIFFERENTIATED_META_UP	62	0.66	2.34	<1.00E-06
CMV_24HRS_UP	61	0.66	2.34	<1.00E-06
MANALO_HYPOXIA_DN	73	0.62	2.33	<1.00E-06
NADLER_OBESITY_UP	57	0.66	2.32	<1.00E-06
IFNA_UV-CMV_COMMON_HCMV_6HRS_UP	20	0.81	2.32	<1.00E-06
SCHUMACHER_MYC_UP	47	0.68	2.32	<1.00E-06
DER_IFNG_UP	54	0.66	2.28	<1.00E-06
IFN_ANY_UP	71	0.61	2.27	<1.00E-06
PEART_HISTONE_DN	63	0.63	2.26	<1.00E-06
IFN_BETA_UP	55	0.64	2.26	<1.00E-06
ADIP_DIFF_CLUSTER4	31	0.72	2.25	<1.00E-06
IFNALPHA_NL_UP	19	0.80	2.25	<1.00E-06
IFN_GAMMA_UP	35	0.69	2.23	<1.00E-06
GOLDRATH_CYTOLYTIC	24	0.75	2.21	<1.00E-06
IFNALPHA_HCC_UP	23	0.74	2.20	<1.00E-06
CANTHARIDIN_DN	45	0.65	2.20	<1.00E-06
MOREAUX_TACI_HI_IN_PPC_UP	43	0.66	2.19	<1.00E-06
DAC_IFN_BLADDER_UP	16	0.82	2.19	<1.00E-06
BENNETT_SLE_UP	19	0.79	2.18	<1.00E-06
STRESS_TPA_SPECIFIC_UP	34	0.69	2.17	2.91E-05
TNFA_NFKB_DEP_UP	17	0.81	2.17	2.84E-05
TARTE_PC	65	0.60	2.17	2.77E-05
BLEO_HUMAN_LYMPH_HIGH_24HRS_UP	86	0.57	2.17	2.71E-05
DSRNA_UP	32	0.69	2.16	2.65E-05
TSA_CD4_UP	24	0.73	2.15	5.32E-05
JECHLINGER_EMT_UP	56	0.61	2.14	1.30E-04
INOS_ALL_UP	47	0.62	2.14	1.27E-04
IFN_ALL_UP	16	0.79	2.14	1.25E-04
IFN_ALPHA_UP	34	0.67	2.13	1.95E-04
LIAN_MYELOID_DIFF_RECEPTORS	33	0.67	2.13	1.91E-04
BRCA_BRCA1_POS	68	0.58	2.13	2.11E-04
ERM_KO_SERTOLI_DN	17	0.78	2.12	2.07E-04
COLLER_MYC_UP	17	0.78	2.12	2.03E-04
AMINOACYL_TRNA_BIOSYNTHESIS	18	0.75	2.10	4.86E-04
PROTEASOMEPATHWAY	21	0.73	2.09	5.20E-04
HSC_INTERMEDIATEPROGENITORS_ADULT	88	0.54	2.09	5.11E-04
PASSERINI_INFLAMMATION	23	0.70	2.08	6.52E-04
LINDSTEDT_DEND_DN	53	0.59	2.07	6.83E-04
ROSS_CBF_MYH	38	0.63	2.07	7.52E-04
LU_IL4BCELL	62	0.57	2.06	7.81E-04
DNA_REPLICATION_REACTOME	41	0.64	2.06	7.68E-04
STRESS_GENOTOXIC_SPECIFIC_DN	36	0.63	2.06	9.11E-04
SERUM_FIBROBLAST_CELLCYCLE	88	0.54	2.05	9.35E-04
YAGI_AML_PROGNOSIS	31	0.65	2.05	9.21E-04
EMT_UP	55	0.58	2.05	9.07E-04

(*Continued*)

Appendix 6. (*Continued*)

Name	Size	ES	NES	FDR q-val
PROTEASOME_DEGRADATION	32	0.65	2.05	9.12E-04
NI2_MOUSE_UP	40	0.62	2.05	9.88E-04
HSC_INTERMEDIATEPROGENITORS_SHARED	80	0.54	2.05	9.74E-04
LINDSTEDT_DEND_UP	44	0.61	2.04	1.05E-03
TRNA_SYNTHETASES	17	0.75	2.03	1.19E-03
SHIPP_FL_VS_DLBCL_DN	30	0.66	2.02	1.29E-03
INSULIN_ADIP_INSENS_UP	17	0.73	2.02	1.36E-03
PROTEASOME	17	0.74	2.01	1.46E-03
GOLDRATH_CELLCYCLE	28	0.65	2.01	1.52E-03
ZHAN_MULTIPLE_MYELOMA_SUBCLASSES_ DIFF	26	0.67	2.01	1.68E-03
YU_CMYC_DN	53	0.58	2.00	1.72E-03
UV-CMV_UNIQUE_HCMV_6HRS_UP	83	0.53	2.00	1.72E-03
CHOLESTEROL_BIOSYNTHESIS	15	0.76	2.00	1.69E-03
TAKEDA_NUP8_HOXA9_3D_DN	20	0.70	2.00	1.69E-03
YU_CMYC_UP	37	0.61	1.99	1.77E-03
UEDA_MOUSE_SCN	86	0.53	1.98	2.20E-03
APOPTOSIS	64	0.55	1.98	2.34E-03
ZELLER_MYC_UP	23	0.68	1.96	3.06E-03
DAC_BLADDER_UP	23	0.67	1.96	3.11E-03
MYC_TARGETS	39	0.58	1.94	3.99E-03
BLEO_MOUSE_LYMPH_HIGH_24HRS_DN	32	0.62	1.94	3.97E-03
CMV_HCMV_6HRS_UP	19	0.70	1.94	3.99E-03
HDACI_COLON_CUR24HRS_UP	28	0.63	1.94	3.96E-03
UNDERHILL_PROLIFERATION	18	0.69	1.93	4.03E-03
MENSSEN_MYC_UP	30	0.63	1.93	4.16E-03
IL1_CORNEA_UP	53	0.55	1.93	4.15E-03
FASPATHWAY	25	0.65	1.93	4.18E-03
MUNSHI_MM_UP	57	0.54	1.92	5.04E-03
IDX_TSA_UP_CLUSTER3	81	0.51	1.92	5.09E-03
ST_TUMOR_NECROSIS_FACTOR_PATHWAY	28	0.64	1.91	5.10E-03
PYRIMIDINE_METABOLISM	55	0.54	1.91	5.39E-03
KNUDSEN_PMNS_UP	65	0.53	1.91	5.40E-03
NFKBPATHWAY	23	0.65	1.90	5.53E-03
HEARTFAILURE_VENTRICLE_DN	56	0.53	1.90	5.62E-03
CMV_UV-CMV_COMMON_HCMV_6HRS_UP	17	0.70	1.90	6.00E-03
ABBUD_LIF_UP	45	0.56	1.88	7.06E-03
HPV31_DN	37	0.57	1.88	7.03E-03
LOTEM_LEUKEMIA_UP	22	0.65	1.88	7.17E-03
TPA_SENS_MIDDLE_UP	55	0.54	1.88	7.59E-03
CASPASEPATHWAY	20	0.67	1.88	7.62E-03
UVC_HIGH_D3_DN	35	0.59	1.87	7.75E-03
WANG_MLL_CBP_VS_GMP_UP	42	0.56	1.87	8.33E-03
MARSHALL_SPLEEN_BAL	25	0.62	1.86	9.11E-03
XU_CBP_UP	25	0.61	1.86	9.64E-03
MUNSHI_MM_VS_PCS_UP	64	0.51	1.86	9.70E-03
GENOTOXINS_ALL_24HRS_REG	22	0.64	1.86	9.65E-03

Abbreviations: ES, enrichment score; NES, normalized enrichment score; FDR, false discovery rate.